Dipole Potentials Indicate Restructuring of the Membrane Interface Induced by Gadolinium and Beryllium Ions

Yuri A. Ermakov,* Alexander Z. Averbakh,* Alexander I. Yusipovich,* and Sergei Sukharev†
*The Frumkin Institute of Electrochemistry, Russian Academy of Sciences, Moscow 117071, Russia, and †Department of Biology, University of Maryland, College Park, Maryland 20742 USA

ABSTRACT The dipole component of the membrane boundary potential, ϕ_d, is an integral parameter that may report on the conformational state of the lipid headgroups and their hydration. In this work, we describe an experimental approach to measurements of the dipole potential changes, $\Delta\phi_d$, and apply it in studies of Be^{2+} and Gd^{3+} interactions with membranes composed of phosphatidylserine (PS), phosphatidylcholine (PC), and their mixtures. $\Delta\phi_d$ is determined as the difference between the changes of the total boundary potential, ϕ_b, measured by the IFC method in planar lipid membranes and the surface potential, ϕ_s, determined from the electrophoretic mobility of liposomes. The Gouy–Chapman–Stern formalism, combined with the condition of mass balance, well describes the ion equilibria for these high-affinity cations. For the adsorption of Be^{2+} and Gd^{3+} to PC membranes, and of Mg^{2+} to PS membranes, the values of $\Delta\phi_b$ and $\Delta\phi_s$ are the same, indicative of no change of ϕ_d. Binding of Gd^{3+} to PS-containing membranes induces changes of ϕ_d of opposite signs depending on the density of ionized PS headgroups in the bilayer. At low density, the induced $\Delta\phi_d$ is negative (−30 mV), consistent with the effect of dehydration of the surface. At maximal density (pure PS, neutral pH), adsorption of Be^{2+} or Gd^{3+} induces an increase of ϕ_d of 35 or 140 mV, respectively. The onset of the strong positive dipole effect on PS membranes with Gd^{3+} is observed near the zero charge point and correlates with a six-fold increase of membrane tension. The observed phenomena may reflect concerted reorientation of dipole moments of PS headgroups as a result of ion adsorption and lipid condensation. Their possible implications to in-vivo effects of these high-affinity ions are discussed.

INTRODUCTION

The layer of polar lipid headgroups separates the apolar hydrocarbon core of the membrane from the surrounding aqueous phase and stabilizes its lamellar structure. Many cellular processes, such as binding and insertion of proteins, lateral diffusion, ligand-receptor recognition, and certain steps in membrane fusion, critically depend on the physical properties of this boundary layer. The intrinsic property of this layer is the presence of ionizable groups, which participate in the ionic equilibrium. Low-affinity cations bind to the negatively charged groups and neutralize a part of the surface charge. Cations with a higher affinity may cause profound effects on the packing of lipids, conformation of headgroups, and the phase state of hydrocarbon chains. Studies in model membrane systems illustrate the ability of mono- and multivalent ions to cause isothermal phase transition in pure lipids, phase separation, and clustering of individual components in mixtures (Boggs, 1987; Hauser, 1991; Graham et al., 1985). In native membranes, which exist in liquid crystalline state, such changes may potentially exert effects on the conformational dynamics of membrane-embedded proteins, and more specifically, on proteins that experience large conformational rearrangements in their transmembrane domains during their functional cycle (Cantor, 1999).

A nonspecific blockage of mechanosensitive channels by Gd^{3+} ions may be a conspicuous example of a lipid-borne effect. Gd^{3+}, a small lanthanide, blocks many types of mechano-gated channels in sub-millimolar concentrations, irrespective of their origin, conductance, or selectivity (Yang and Sachs, 1989; Hamill and McBride, 1996). Early attempts to understand this property of Gd^{3+} implied the presence of specific motifs common to these proteins that may be targeted by the ion with high affinity. Another explanation to such generalized effect may be binding of Gd^{3+} to the lipid component of the cell membrane and alteration of the physical properties of the bilayer surrounding the channels. The high-affinity binding of lanthanides has been known to affect physical properties of phospholipid bilayers by causing phase transitions (Hammoudah et al., 1979; Li et al., 1994; Verstraeten et al., 1997), liposome fusion (Bentz et al., 1988), and pore formation in erythrocytes (Cheng et al., 1999).

Previous data (Ermakov et al., 1992) indicated that Be^{2+}, another small cation, is characterized with a higher affinity to phosphatidylcholine membranes compared to other divalent cations. It has been known for toxicity, which is manifested primarily as abnormal immune reactions causing lesions in lungs in response to inhaled Beryllium dust. This cation was recently shown to induce apoptosis in several macrophage cell lines (Sawyer et al., 2000). It appeared timely to study the interaction of Be^{2+} with the negatively charged lipid phosphatiylserine, which has recently been shown to be an important marker on the surface of apoptotic cells, recognizable by macrophages (Fadok et al., 1998, 2000).

Received for publication 5 July 2000 and in final form 6 January 2001.
Address reprint requests to Sergei Sukharev, Department of Biology, Bldg 144, University of Maryland, College Park, MD 20742. Tel.: 301-405-6923; Fax: 301-314-9358; E-mail: ss311@umail.umd.edu.

0006-3495/01/04/1851/12 $2.00

In the present work, we take electrostatic approach to study high-affinity interactions of Be^{2+} and Gd^{3+} ions with membrane surfaces. The traditional electrokinetic method widely used for determination of ion binding to membrane surfaces does not provide complete information on the structure of membrane–water interface because it "senses" only changes in the diffuse part of the double layer, outside of the membrane. The inner, dipole component of the boundary potential is a parameter directly related to the chemical structure of the interface, orientation, and hydration of the polar headgroups (Gawrisch et al., 1992). Measurements of the dipole potential may provide additional information complementary to "local" structure usually studied by the infrared or NMR spectroscopic techniques (Hauser, 1991). Here, we present a detailed description of experiments, procedures, and quantitative analysis that allow us to distinguish the effects of cations of different affinity, Mg^{2+}, Be^{2+}, and Gd^{3+}, on the surface and dipole components of the boundary potential in membranes of different compositions. For this purpose, we combine electrokinetic measurements of the surface potential, with the intramembrane field compensation (IFC) method specially designed for monitoring changes of the total boundary potential, including its dipole component. We show the equivalence of the IFC and electrokinetic methods in detection of low-affinity interactions as illustrated by Mg^{2+} adsorption on phosphatidylserine (PS). We find that Be^{2+} and Gd^{3+} ions characterized with high affinity may exert significant effects of both signs on the dipole potential at the boundary, dependent on the lipid composition of the bilayer and pH. We observe the most profound effect of Gd^{3+} and Be^{2+} specifically on the dipole potential of PS membranes, which in the case of Gd^{3+} correlates with changes of mechanical properties of the lipid bilayer.

MATERIALS AND METHODS

Principles of measurements

To study the electric field distribution across the membrane, we use the combination of the traditional electrokinetic technique applied to suspensions of liposomes with the intramembrane field compensation (IFC) method. The mobility of liposomes in the electric field provides information about the electric charge and potential drop in the diffuse part of the double layer termed surface potential, ϕ_s. The IFC technique, in contrast, permits measurements of the difference of total boundary potentials between the two sides of the planar bilayer lipid membrane (BLM). The changes of total boundary potential, $\Delta\phi_b$, observed upon a unilateral ion adsorption are compared with changes of the surface potential ϕ_s obtained on liposomes of the same composition. The difference $\Delta\phi_b - \Delta\phi_s$ is attributed to the variation of the dipole component of the boundary potential, $\Delta\phi_d$.

Measurement of the surface potential

Surface potentials, ϕ_s, were calculated from the electrophoretic mobilities of lipososmes, assuming the distance of the shear plane from the physical boundary, $\delta = 0.2$ nm (McLaughlin, 1989). The classical Gouy–Chapman–Stern (GCS) model was combined with the Langmuir isotherm (McLaughlin et al., 1981), which took into account the competition of Be^{2+} or Gd^{3+} with cations of the background electrolyte and, in some instances, with protons. The maximal density of negatively charged binding sites always corresponded to the packing of PS in the bilayer (0.6 nm^2 per lipid molecule, or charge density $S = 0.2$ C/m^2), and the stoichiometry of ion–phospholipid binding was assumed 1:1. To describe quantitatively high-affinity interactions of the ions with negatively charged membrane surfaces and to account for the possible effect of bulk depletion, we included the condition of mass balance to the set of equations (see Appendix for details).

Boundary potential: the intramembrane field compensation method

The advantage of BLM as experimental system is the accessibility of both sides of membrane-to-surface modifications and changes of bath composition. The voltage drop across each membrane–water interface (total boundary potential, ϕ_b) is a sum of the diffuse part of the electric double layer (surface potential, ϕ_s) and the internal dipole component, ϕ_d. Under short-circuit conditions, when the electric potential in the bulk solutions on both sides of BLM is the same, the voltage drop across the membrane core (intramembrane field) is equal to the difference of boundary potentials on each side. It has been known that the membrane capacitance depends on the applied voltage and has a minimum when the intramembrane field is zero (Babakov et al., 1966; Alvarez and Latorre, 1978; Cherny et al., 1980). We use this property of the "zero-field point" to measure the difference of boundary potentials between the two sides of the membrane by compensating the intramembrane field with an externally applied voltage. The dependence of membrane capacitance on voltage was modeled either as electrostriction of an elastic capacitor (Passechnik and Hianik, 1978; Schoch et al., 1979; Shimane et al., 1984), or as change in membrane area due to increase of the amplitude of thermal undulations with voltage (Leikin, 1985). Irrespective of the physical model, the voltage-dependence of capacitance C may be approximated near its minimum, C_0, by a parabola,

$$\frac{C}{C_0} = 1 + \alpha U^2 \approx 1 + \frac{\Delta h}{h_0}, \qquad (1)$$

where U is the voltage across the membrane core (intramembrane field), $\alpha \equiv C_0/2h_0k$ is the "compliance" of the elastic capacitor with the modulus k and the distance between the plates h_0. When the voltage $U = U_0 + U_1 \sin \omega t$ is applied to the elastic capacitor, the current $j = dCU/dt$ has three harmonics (Carius, 1977; Hianik and Passechnik, 1995),

$$j = \omega C U_1 \{[1 + 3\alpha U_0^2 + \tfrac{3}{4}\alpha U_1^2]\cos \omega t + 3\alpha U_1^2 U_0 \sin 2\omega t - \tfrac{3}{4}\alpha U_1^2 \cos 3\omega t]\}. \qquad (2)$$

The equation shows that, at $U_0 = 0$, the capacitance is minimal and the amplitude of the second harmonic becomes zero. This corresponds to a symmetrical membrane, or to a state in which the intramembrane field is completely compensated. Note that the amplitude of the third harmonics is independent of U_0 and is proportional to α, which is effective mechanical compliance of the membrane to electrostriction (Alvarez and Latorre, 1978; Schoch et al., 1979; Cherny et al., 1980; Leikin, 1985; Hianik and Passechnik, 1995). The experimental procedure of the IFC, with an automatic minimization of membrane capacitance, was first introduced by Sokolov and Kuzmin (1980). The method is implemented with a circuit containing a lock-in detector of the second harmonic. The dc output from the detector is continuously recorded and fed with a proper phase back to the membrane. The dc bias automatically minimizes the capacitance and thereby keeps the intramembrane field at zero. In practice, the procedure

works well when the real (ohmic) component of the membrane current is small compared to the capacitive component. This condition is satisfied at sufficiently high frequency of the fundamental harmonic $f = 1/2\pi\omega$.

The IFC method detects the difference of boundary potentials, $\Delta\phi_b$, between the two sides of the membrane. In contrast to the traditional method of ϕ_b measurement using permeant hydrophobic ions (Andersen et al., 1976), IFC is less sensitive to changes in membrane fluidity. Initially, in a symmetric membrane $\Delta\phi_b = 0$. A unilateral introduction of ions changes the boundary potential at the *cis*-side only, producing $\Delta\Delta\phi_b$. Because the boundary potential of the opposite (*trans*-) side remains constant, it can be used as reference, and the change of the boundary potential on the *cis*-side must be equal to the measured difference of boundary potentials between the two sides, $\Delta\phi_b$.

The automatic IFC procedure described above is highly advantageous for continuous monitoring of adsorption and desorption of charged molecules on one side of a planar membrane. By keeping the intramembrane field close to zero, the experimenter may avoid electric breakdown of the BLM when the difference of boundary potentials between the sides is high. We should note that, in the case of unilateral adsorption of Gd^{3+} on PS membranes, the observed $\Delta\phi_b$ can be as high as 350 mV.

Experimental procedures

Multilayer liposomes were prepared by a conventional technique. Lipids in chloroform were dried under vacuum for 30 min in a round-bottom flask on a rotor evaporator. The lipid film was then rehydrated in the background electrolyte of a desired composition for 10 min, and than the flask was shaken by hand until a homogeneous suspension was obtained. The optimal concentration of lipids for electrokinetic measurements in our experiments was 1 mg/ml. Typically, the ions of interest were added to the prepared liposomes before measurements. The concentration of the introduced ion was varied from low to high with a series of sequential additions of concentrated stock solutions. The exact compositions of electrolytes in each experiment are listed in figure legends. The electrophoretic mobility of liposomes was measured on a photon correlation spectrometer Zetasizer-2 (Malvern Instruments, Worcestershire, UK). The output from a single run was the main frequency of the final spectrum, which is linearly related to the electrophoretic mobility μ and ζ-potential (Uzgiris, 1978; Hunter, 1981).

Planar lipid membranes were formed on the aperture of 1 mm^2 in the septum of a Teflon chamber from lipid solutions in decane (15 mg/ml). All lipids (bovine PS and egg phosphatidylcholine, PC) were purchased from Avanti Polar Lipids Inc. (Alabaster, AL) or from Sigma (St Louis, MO) and used without further purification. All salts were of reagent grade (Aldrich, Milwaukee, WI) and the buffers (see legends) were prepared with double distilled water.

The experimental setup for IFC measurements includes a conventional sine-wave generator, a current-to-voltage converter (model 181, Princeton Applied Research, Princeton, NJ), a first harmonic rejection RC-filter, narrow-band amplifiers for the 2nd and 3d harmonics, a lock-in amplifier (model 126, Princeton Applied Research), digital voltmeters, and a chart recorder. The ac (20 mV, 272 Hz) and dc voltage components were summed with an operational amplifier and applied to the membrane with Ag/AgCl electrodes, either directly or via salt bridges. $GdCl_3$ or $BeSO_4$ were manually introduced to the *cis*-compartment of the chamber with continuous stirring of the buffer. In some experiments, the solution in the *cis*-compartment was exchanged with a two-channel peristaltic pump (Microperpex 2132, LKB, Sweden) allowing for a precise balance of the buffer inflow and outflow.

Membrane tension was assessed by applying gradients of hydrostatic pressure with simultaneous measurements of the capacitance, which is proportional to the area of the black part of the BLM. The membrane bulged under the pressure gradient was treated as a spherical cap, and the tension, γ, was calculated with the equation that includes the membrane capacitance C, its variation ΔC, the specific value, C_s (0.5 $\mu F/cm^2$) and the hydrostatic pressure across it, all related by the law of Laplace:

$$\gamma = \frac{\rho g \Delta h}{4\sqrt{\pi C_s}} \frac{C}{\sqrt{\Delta C}}. \quad (3)$$

RESULTS

Low-affinity ion–membrane interactions: a comparison of IFC with electrophoresis

After the planar membrane is formed in a symmetrical electrolyte and its capacitance stabilizes, the difference of boundary potentials between the two sides, $\Delta\phi_b$, measured by IFC is usually close to zero (0 ± 3 mV). Introduction of inorganic multivalent cations to the *cis* compartment generates $\Delta\Delta\phi_b$ (further denoted as $\Delta\phi_b$), with the sign corresponding to a positive shift of the surface potential on the *cis* side of BLM. An extensive perfusion of the *cis* compartment with the background electrolyte returns $\Delta\phi_b$ to zero. These experiments convinced us that interaction of ions with the membrane surface is completely reversible for all ionic species studied here. The boundary potential of the *trans* side, therefore, remains constant throughout the experiment (i.e., for 1–1.5 hr), suggesting that cations do not permeate through the membrane, and all changes of the potential measured by IFC are restricted to the *cis* side.

Interaction of Be^{2+} with uncharged lecithin membranes results in significant positive shifts of the ζ- and boundary potentials, as shown by both electrokinetic and IFC measurements (Fig. 1). At low concentrations, ζ-potentials essentially coincide with $\Delta\phi_b$. Unlike $\Delta\phi_b$, ζ-potential exhib-

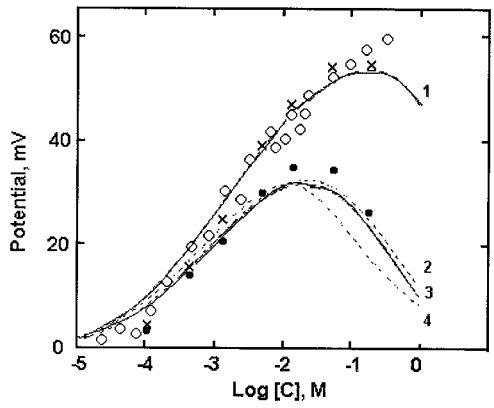

FIGURE 1 Electrostatic effects of Be^{2+} binding to phosphatidylcholine membranes. The surface potential (*crosses*) was calculated from ζ-potentials (*filled circles*) according to Eq. A2 with the parameter $x = \delta = 0.2$ nm. The changes of the total boundary potential were measured with IFC (*open symbols*). Both types of measurements were done in 0.1 M KCl, 20 mM imidazole, pH 6.4. The theoretical curves for the surface (*curves 1 and 2*) and ζ-potential (*curves 3 and 4*) were calculated according to the GCS model using the isotherm (Eq. A7) with parameters $S = 0.2$ C/m^2, $K_2 = 400$ M^{-1} (*curves 1 and 3*); $S = 2$ C/m^2, $K_2 = 40$ M^{-1} (*curve 2*); $S = 0.02$, C/m^2, $K_2 = 4000$ M^{-1} (*curve 4*). The data set shown with open symbols is reproduced from Ermakov et al. (1994), with permission.

its a maximum in the range of Be^{2+} concentrations between 10 and 100 mM. Taking into account the position of the shear plane ($\delta = 0.2$ nm) in Eq. A2 (see Appendix), we calculated the surface potentials from ζ-potentials. After such transform, we observe no difference between the data obtained with the two methods. The theoretical curves for ζ and surface potentials (*solid lines*), calculated according to the GCS model (Eqs. A2–A5 and A7) using the same parameters, correspond well to both sets of experimental points (Ermakov et al. 1994).

We presume that the maximum of ζ- potential curve in Fig. 1 is a result of two processes, the surface potential increase due to the cation adsorption, followed by the decline due to self-screening by the electrolyte. A similar nonmonotonous character of ζ-potential dependencies on divalent ion concentration has been reported previously (Tatulian, 1993). The GCS model predicts that, at a high ionic strength, the effect of screening is much more pronounced at a distance from the charged surface compared to that at the surface itself. Thus, the ζ-potential shows the maximum at lower concentrations than the surface potential, ϕ_s. By fitting the ζ and ϕ_s curves to the model, we obtain $\delta = 0.18$ nm, which independently confirms previous estimates of the shear plane distance (for review see McLaughlin, 1989). A good correspondence of the data between the electrokinetic and IFC techniques strongly suggests that interaction of Be^{2+} with the surface of PC membranes induces changes in the diffuse part of the electric double layer only. On the assumption of the 1:1 binding stoichiometry for Be^{2+}-PC, the data presented in Fig. 1 predict the binding constant of 400 M^{-1}. The electrostatic effects reported for other divalent cations (Ca^{2+}, Mg^{2+}, Sr^{2+}, Ba^{2+}) do not exceed 15 mV (Tatulian, 1993, 1999). The binding constants were calculated in the referenced paper on the assumption of a different stoichiometry. When the 1:1 stoichiometry is applied to these data, the binding constants for these cations are found two orders of magnitude less than that for Be^{2+} (McLaughlin et al., 1978).

In this study, we use Mg^{2+} as a low-affinity ligand to compare its effects with those of high-affinity ions. The data illustrating the Mg^{2+} adsorption on negatively charged membranes made of PS obtained with the two methods are shown in Fig. 2. The curve for surface potentials is similar to those previously published (McLaughlin et al., 1981; Ermakov et al., 1992). The binding constant found from the zero charge point is 4 M^{-1}, indicating very low affinity. The second set of data obtained with IFC shows the variation of the boundary potential, $\Delta\phi_b$. To compare how the two potentials change with concentration, we represent $\Delta\phi_b$ in the same scale as ϕ_s. For this purpose, we offset the IFC data by the value of initial surface potential determined from the ζ-potential of PS liposomes measured in the pure background electrolyte. Here, we assume that the surface component, ϕ_s, is the same for planar bilayers and liposomes of the same composition. As previously, ϕ_s is obtained from ζ-potentials using Eq. A2 with the parameter $\delta = 0.2$ nm. Under experimental conditions given in Fig. 2, the initial value for ϕ_s is -85 mV. Both data sets coincide and demonstrate good correspondence with the GCS model, indicating that the changes of the boundary potential take place only in the diffuse part of the double layer, leaving the dipole potential unchanged. The theoretical curve (Fig. 2, *solid line*) calculated according to the adsorption isotherm (Eq. A6) has the predicted maximal slope of 28 mV per decade.

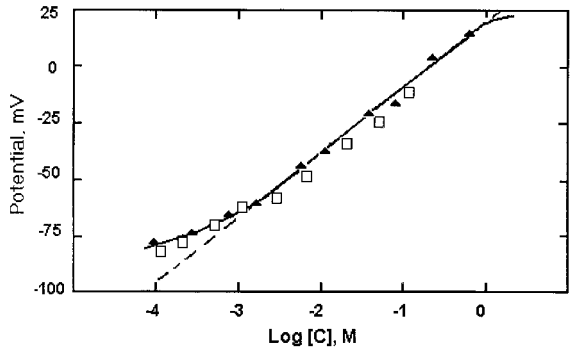

FIGURE 2 Binding of Mg^{2+} to PS membranes. The data for the surface (*filled symbols*) and boundary potentials were obtained in 0.1 M KCl, 20 mM imidazole, pH 6.4. The entire data measured with IFC (*open symbols*) were offset for -85 mV, which corresponds to the surface potential of liposomes without Mg^{2+}. All surface potentials here and below were calculated from electrokinetic data with the account for the shear plane distance $\delta = 0.2$ nm. The theoretical curve (*solid line*) and its asymptote (*dashed line*) were calculated according to Eq. A6 with parameters $S = 0.2$ C/m^2, $K_1 = 0.2$ M^{-1} for K^+ and $K_2 = 4$ M^{-1} for Mg^{2+}.

The dipole component in the presence of ions with high affinity

The data of the two methods illustrating the adsorption of Be^{2+} on PS membranes are represented in the same surface potential scale in Fig. 3. The curves have different shapes compared to that for Mg^{2+}, and show a noticeable discrepancy between the two methods. The maximal magnitude of the boundary potential change is about 35 mV higher. Both curves ($\Delta\phi_b$ and ϕ_s) display the maximal slope, significantly exceeding the expected slope for divalent cations, apparently due to bulk depletion of Be^{2+}. To describe this observation quantitatively, we supplemented the GCS model (Eqs. A2, A4–A6) with the condition of the material balance (Eqs. A8–A10). A theoretical curve (Fig. 3, *dashed line*) was generated with parameters $c_{lip} = 0$ (no depletion) and $K_2 = 10^3$ M^{-1}. Another curve (*solid line*), which illustrates depletion at low Be^{2+} concentrations, corresponds to $c_{lip} = 1$ mM, the amount of lipid used in the electrokinetic experiment. The latter is in good agreement with the initial part of the experimental curve. Note that the amount of lipid introduced into the bilayer chamber during

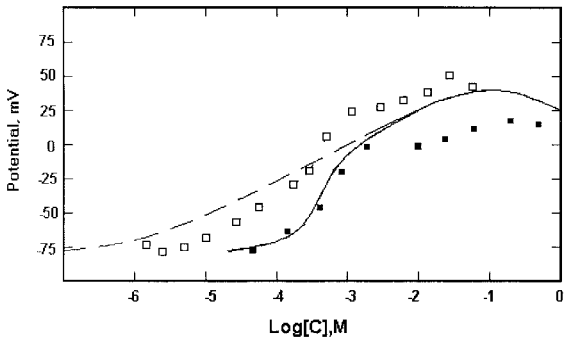

FIGURE 3 Binding of Be^{2+} to PS membranes. Open symbols show IFC data for boundary potentials offset for −85 mV, which corresponds to the initial ϕ_s in the background electrolyte; closed symbols represent surface potentials calculated from electrokinetic data. Experimental conditions were as in Fig. 2. Theoretical curves were calculated according to Eq. A6 with binding constants $K_1 = 0.6\ M^{-1}$ for K^+, and $K_2 = 1000\ M^{-1}$ for Be^{2+} and with $c_{lip} = 0$ (*dashed line*) and $c_{lip} = 1$ mM (*solid line*).

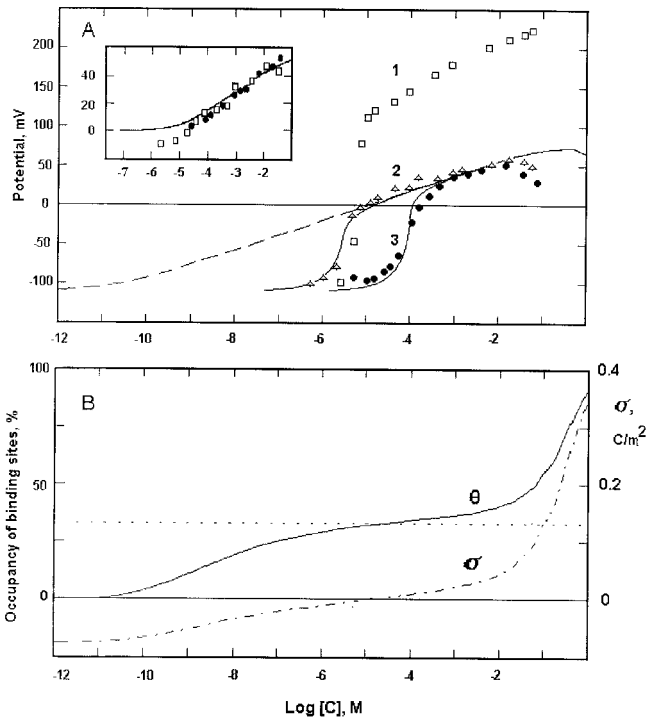

FIGURE 4 Binding of Gd^{3+} to membranes made of PS, PC and their mixtures. (*A*) Boundary and ζ-potentials were measured with membranes made from 100% PS (*1* and *3*) and from the mixture PS:PC = 3:2 (*2*) (10 mM KCl, pH 7.1). The data are presented against the total concentration of $GdCl_3$ in the chamber. The IFC data (*open symbols*) are offset by −114 mV for pure PS (*squares*) and for −101 mV for the mixture (*triangles*). The surface potentials obtained from electrokinetic data are shown by closed symbols. *Inset*: Gd^{3+} binding to membranes made of pure PC. The symbolic notation of is the same as previously. All theoretical curves are calculated in the framework of GCS model (Eqs. A2, A4, A5) taking into account the competitive binding of Gd^{3+} and K^+ to PS (Eq. 6, $K_1 = 4$, $K_2 = 5 \cdot 10^4\ M^{-1}$, respectively) and Gd^{3+} to PC (Eq. A7, $K_2 = 10^3\ M^{-1}$). The parameter c_{lip} in the condition of mass balance (Eq. A8) is 0 (*dashed line*), 0.02, and 0.3 mM for curves 2 and 3, respectively. (*B*) The surface charge density, σ, and occupancy of binding sites, Θ, calculated for pure PS (50 mM KCl, pH 7.0, $K_1 = 1\ M^{-1}$, $K_2 = 5 \cdot 10^4\ M^{-1}$, $c_{lip} = 0$). The dotted line indicates the level of 33% occupancy corresponding to the zero charge point.

membrane formation is typically less than that used in electrophoretic measurements, but is more difficult to control. At lower c_{lip}, the steepest region of the corresponding theoretical curve is expected to be shifted leftward. The shape of the $\Delta\phi_b$ curve suggests that the depletion also takes place in the IFC experiment. At higher Be^{2+} concentrations, the experimental curves for ϕ_s and $\Delta\phi_b$ have plateau-like regions, not predicted by the theory. The surface potential obtained from electrokinetic data levels at ~0 mV, whereas the boundary potential plateaus at +30–35 mV. This difference can be attributed to the increase in the dipole component of the boundary potential in PS membranes in the presence of Be^{2+}.

Experiments with Gd^{3+} revealed much more pronounced effects on the boundary dipole component. Figure 4 *A* shows the IFC and electrokinetic data obtained with Gd^{3+} in membranes made of PS. As in the previous case with Be^{2+}, the data of the two methods represented in the same scale are significantly different. All curves display a region of steep rise of the potential; in IFC experiments, it takes place at lower Gd^{3+} concentrations. The most drastic difference is observed in the magnitude of the effects; the maximal increase of ϕ_s is for 160 mV, whereas ϕ_b changes for up to 350 mV. Such large effects of Gd^{3+} on ϕ_b are observed at neutral pH on pure PS only. Mixing PS with PC (to 60–80 mol% PS in the mixture) changes $\Delta\phi_s$ slightly, but strongly diminishes the maximal $\Delta\phi_b$. Note that, in membranes made of pure PC, the changes of ϕ_s and ϕ_b coincide in the entire range of concentrations (see Fig. 4 *A*, *inset*), similar to what was observed with Be^{2+} (Fig. 1). This suggests that the changes of the boundary potential in the latter case are restricted to the diffuse part of the double layer.

Theoretical curves in Fig. 4 *A* are generated using binding constants of Gd^{3+} to PS and PC of $5 \cdot 10^4$ and 10^3, respectively. The dashed curve in Fig. 4 *A* is built in the framework of the traditional GCS model ($c_{lip} = 0$); the two solid curves are computed with the same binding parameters, but account for Gd^{3+} depletion with parameters c_{lip} of 0.02 mM (*curve 2*) and 0.3 mM (*curve 3*), respectively. These curves well approximate the electrokinetic data (*curve 3*) and IFC data obtained in membranes made with 60% PS in mixture with PC (*curve 2*). In the latter case, the amplitude of the IFC signal does not exceed ϕ_s, and the right part of the $\Delta\phi_b$ curve coincides with the curve predicted according to the GCS theory, suggesting that adsorption of Gd^{3+} in this particular case affects only the diffuse component of the boundary potential. Large $\Delta\phi_b$ obtained in pure PS membranes that drastically exceed ϕ_s, cannot be explained in the framework of the GCS model and indicates

a significant increase of the dipole component. To study the onset of this positive dipole effect and to avoid the effect of bulk depletion, we performed a series of experiments, in which the concentration of Gd^{3+} near the membrane was "clamped" at concentrations between 10^{-8} to 10^{-2} M by perfusing large volumes of Gd^{3+}-containing buffers (at least 10 chamber volumes). The results revealed a sudden change of the boundary potential at $\sim 10^{-6}$ M Gd^{3+}, just below the zero charge point (data not shown).

Using the same set of parameters in the model, we calculated the variations of the surface charge density, σ, and the occupancy of binding sites by Gd^{3+}, Θ, on PS membranes as a function of bulk Gd^{3+} concentration (Fig. 4 *B*). At low concentrations (10^{-11}–10^{-7} M), a relatively steep increase of Θ reflects the substitution of K^+ ions of background electrolyte at the binding sites by Gd^{3+}. In the middle part (10^{-6}–10^{-2} M), the occupancy varies insignificantly, staying close to the zero charge point ($\Theta = 33\%$). Only at submolar concentrations, the range that is difficult for experimentation, Θ grows steeply and then saturates. The surface potential (Fig. 4 *A*, *dashed line*) changes almost linearly with the log of [Gd^{3+}]. This asymptotic behavior with the slope of 20 mV/decade is dictated by the Boltzmann relationship (Eq. A5), which predicts the concentration of cations near the charged surface, $c(0)$, practically independent on their bulk concentration and the slowly changing charge density at the surface. This phenomenon reflects merely the screening of surface charge by trivalent cations. The curves clearly illustrate the tendency of the system to stay close to the point of electroneutrality at intermediate concentrations of the adsorbed ion.

At higher concentrations of Gd^{3+}, outside of the range of depletion, the experimental curves obtained with both methods have similar shape (Fig. 4 *A*). We used these data subsets to quantify the effects of Gd^{3+} on the dipole component. Two series of experiments were designed to study the Gd^{3+}-induced dipole potential as a function of density of ionized PS in the membrane. One series resulted in pairs of ϕ_s and $\Delta\phi_b$ data taken for different PS/PC mixtures under equal experimental conditions. In another series, the carboxyl groups of PS were titrated with an acid, thus the measurements was taken on pure PS membranes at pH ranging from 2.8 to 7.0. In the latter case, the competitive binding of H^+, K^+, and Gd^{3+} was taken into account in calculations of surface potentials. The surface potentials determined from electrokinetic data and the parameters used in calculations are given in Table 1. As previously, we subtracted ϕ_s from $\Delta\phi_b$ at every Gd^{3+} concentration to determine the change of the dipole component. For this purpose, we used the surface potential, ϕ_s, after its correction for the proper value of c_{lip}, adjusted as a free parameter, such that the regions of the steepest slope for both $\Delta\phi_b$ and ϕ_s curves coincide. (Technically, we could use a theoretical approximation of ϕ_s [Fig. 4 *A*, *dashed line*], the position of which, in the $\phi_s - \log C$ graph, is determined only by the binding constant for Gd^{3+} and density of binding sites.) The changes of the dipole component $\Delta\phi_d = \Delta\phi_b - \phi_s$, obtained with membranes made from different PS/PC mixtures, are represented in Fig. 5 *A*. The right part of the curve for pure PS exhibits a shallow linear slope as the Gd^{3+} concentration increases. All other data show no systematic dependence on Gd^{3+} concentration. The points obtained with pure PC are scattered strictly around zero mV. A similar $\Delta\phi_d$ graph was built for PS membranes studied at different pH (Fig. 5 *B*). The mean values of $\Delta\phi_d$ found from the right sides of the $\Delta\phi_d - \log[Gd^{3+}]$ graphs are presented in Fig. 6 as a function of density of negatively charged binding sites relative to its maximal value in pure PS at pH

TABLE 1 Parameters used for quantitative treatment of electrokinetic data according to the GCS model

1	2	3	4	5	6	7
S/S_{max}	PS (%)	ϕ_s (mV)	c_{lip} (mM) 10 mM KCl, pH 7.1, $K_1 = 4\ M^{-1}$	pH	ϕ_s (mV)	c_{lip} (mM) 50 mM KCl, $K_1 = 1\ M^{-1}$
1.0	100	−114	0.02	7.1	−89	0.1
0.8	80	−108	0.08			
0.78	(100)			4.32	−84	0.015
0.6	60	−101	0.01			
0.54	(100)			3.8	−75	0.02
0.4	40	−92	0.025			
0.29	(100)			2.85	−59	0.01
0.2	20	−71	0.03			

Columns 1 and 2 represent the density of negatively charged binding sites, S/S_{max}, and the membrane composition (%PS), are common for the two series of experiments. In the first series (columns 3 and 4), the density was varied only by changing the PS:PC ratio in the lipid mixture. The second series (columns 5–7) shows the results of titration of the surface of pure PS membranes at different pH. c_{lip} is the putative concentration of lipid in the BLM chamber in reciprocal IFC experiments used as an adjustable parameter. The Gd^{3+} binding constants to PS and PC were $K_2^{PS} = 5 \cdot 10^4\ M^{-1}$, $K_2^{PC} = 10^3\ M^{-1}$, respectively; pK for PS headgroup protonation was 3.0, and the binding constants for K^+ to PS (K_1) are listed in columns 4 and 7. The values of initial ϕ_s (columns 3 and 6) were used to represent the IFC and electrokinetic data in the same scale and evaluate changes of dipole potential in the two series of experiments (Fig. 5).

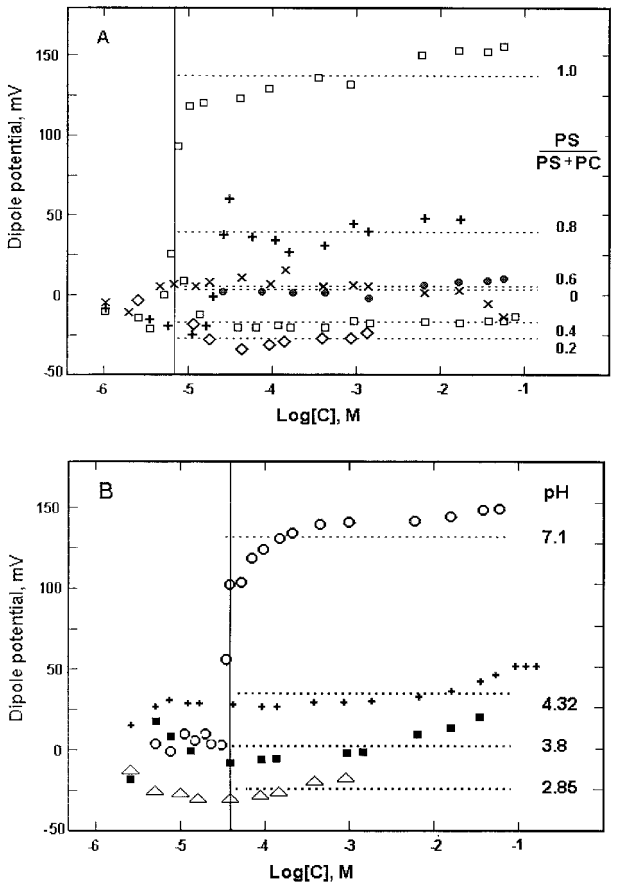

FIGURE 5 Changes of the dipole potential induced by Gd^{3+} adsorption on membranes made from (*A*) different PS/PC mixtures (10 mM KCl, pH 7.1) and on membranes made of (*B*) pure PS at different pH (50 mM KCl). The boundary potential changes were measured by IFC method and offset by the value of surface potential calculated according to the GCS model with parameters listed in Table 1. For calculation of mean values of the dipole potential (*dotted lines*), we use data points to the right of the vertical dividing line. The position of this line corresponds approximately to the region of the steepest slope for most of the experimental ϕ_b curves.

7.0 ($S = 0.2$ C/m^2). Independent of the method of varying the density of the ionized form of PS, we observe the same changes of the dipole component of the boundary potential induced by Gd^{3+}. At low densities (<60%), we see a negative change of the dipole potential of about 30 mV. At the highest density achieved with pure PS and neutral pH, the maximal magnitude of effects is +140 mV. The sign "+" means that the change of the dipole component augments the change of the surface component upon adsorption of positively charged ions and increases the absolute value of the outwardly directed dipole. Note that the two series of experiments were performed at different ionic strength of the background electrolyte (10 or 50 mM KCl), yet the magnitude of the dipole effect was the same. This indicates that the changes of electric potential take place in the unscreenable part of the double layer, i.e., inside the membrane. A large positive dipole effect of Gd^{3+} clearly correlates with a high contents of negatively charged PS in the bilayer.

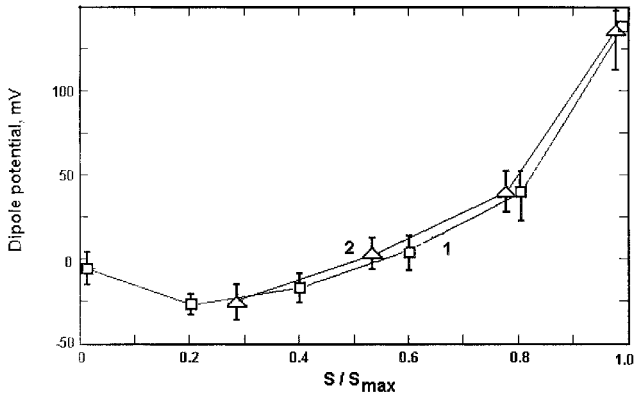

FIGURE 6 The mean values of dipole potentials induced by Gd^{3+} adsorption on membranes with different density of negatively charged binding sites, S, normalized to the maximal value $S_{max} = 0.2$ C/m^2 corresponding to pure PS at pH 7.0. The squares represent the data for different PS/PC mixtures (Fig. 5 *A*), the triangles are the data for pure PS measured at different pH (Fig. 5 *B*).

One possible reason for the dipole potential change may be binding of cations at the plane beneath the layer of negatively charged headgroups. The sign of the effect in this case should be the same as observed in experiments, but the magnitude is expected to be proportional to the density of adsorbed Gd^{3+} ions, analogous to the density-dependent dipole effect of 1-anilino-8-naphtalenesulfonate (Ermakov et al., 1983). Figure 7 shows combined data for ϕ_d obtained for pure PS at two different ionic strengths and presented as a function of the occupancy, Θ, calculated from the model that accounts for bulk depletion. The experimental points consistently deviate from the hypothetical linear dependence (*dashed line*); they show that ϕ_d undergoes stepwise

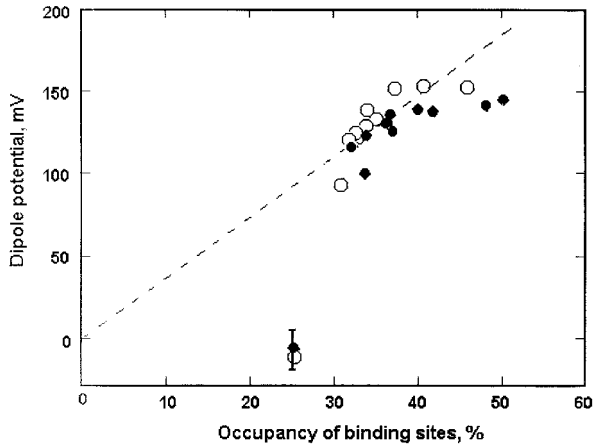

FIGURE 7 The dipole potential versus the occupancy of binding sites by Gd^{3+} cations calculated for experiments with membranes made of pure PS. The data sets are the same as in Fig. 5. Background electrolyte was 50 mM KCl (*filled circles*) and 10 mM KCl in all other experiments, pH 7.0.

increase near the zero charge point ($\Theta \approx 30\%$), remaining constant at higher occupancies.

Mechanical properties of the bilayer

Our experimental setup permitted simultaneous recording of the first three harmonics of the capacitive current, which report on the capacitance itself, electrical asymmetry of the membrane, and its compliance to electrostriction, respectively (see Materials and Methods, Eq. 2). Adsorption of Gd^{3+} had no visible effect on the BLM capacitance (represented by the 1st harmonic), however we consistently observed a decrease of the amplitude of the third harmonic. The parameter α proportional to the ratio of the first and third harmonics, which reflects the compliance of the membrane to electrostriction, also declined. The major change in α was observed at Gd^{3+} concentrations of $\sim 10^{-7}$ M (i.e., about two orders of magnitude lower than the zero charge point), where the electrostatic effects are small. In the range of 10^{-6}–10^{-5} M Gd^{3+}, the membrane seems to be very rigid, such that the amplitude of the third harmonic becomes comparable to the noise level (data not shown). For this reason, we can correlate the changes of α neither with the density of absorbed ions, nor with the onset of the dipole effect.

In the presence of Gd^{3+}, we observed a strong increase of membrane tension, γ, for BLMs made with PS, but not with PC (Fig. 8). Tensions were determined from relative expansions of the BLM measured as an increase of capacitance, $\Delta C/C$ under different hydrostatic gradients (see Eq. 3). Note that solvent-containing bilayers can expand because of incorporation of an extra lipid material from the surrounding meniscus. The calculated tension remains practically constant as the relative membrane expansion increases (Fig. 8 *A*). The mean values for tensions obtained at different Gd^{3+} concentrations are plotted in Fig. 8 *B*. The PC membranes are characterized with the relatively low tension ($\sim$0.2 mN/m), essentially independent on the Gd^{3+} concentration. The same independence of Gd^{3+} exhibit membranes made of PS mixed with PC (60% PS). For membranes formed of pure PS, the tension rises at $\sim 10^{-5}$ M Gd^{3+}, i.e., in the range of concentrations where the dipole potential steeply increases, which approximately corresponds to the zero charge point. The maximal increase of BLM tension is about 6 times over the control.

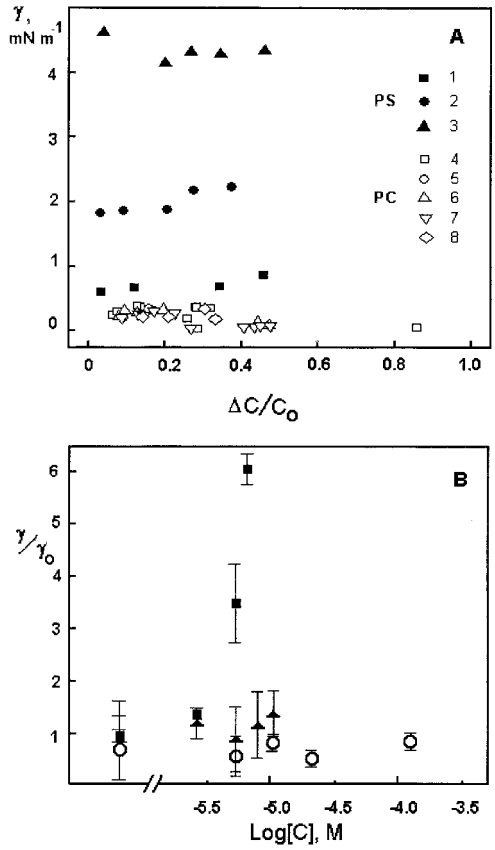

FIGURE 8 Surface tension of planar lipid membranes made from PC (*open symbols*) and PS (*closed symbols*) in the presence of Gd^{3+}. The tension was determined by capacitance measurements under different hydrostatic pressure gradients between *cis* and *trans* compartments. (*A*) The tension of BLM plotted as a function of relative membrane expansion (measured as changes of BLM capacitance, $\Delta C/C_o$). The concentrations of Gd^{3+} are 0, 5, 7.5 μM (membranes from PS, *curves 1–3*) and 0, 5, 10, 20, 120 μM (membranes from PC, *curves 4–8*), respectively. (*B*) The relative changes of BLM tension at different total Gd^{3+} concentrations on the *cis*-side of the chamber. The BLM tension in the background electrolyte (10 mM KCl, pH 7.1) was taken as unity. Triangles represent the data for 60% of PS in the PS/PC mixture.

DISCUSSION

We demonstrate that Be^{2+} and Gd^{3+} ions exert dipole effects at the interfaces of PS-containing membrane. We come to this conclusion by comparing the changes of the total boundary potential with changes of its surface component, measured with the IFC method and electrophoretic technique, respectively. Although the physical principles of the measurements are completely different, the data obtained on Be^{2+} or Gd^{3+} with PC, and Mg^{2+} with PS, membranes (Figs. 1, 2, and 4 *A*, *inset*) show a remarkable agreement of the two methods. These examples of low-affinity interactions illustrate the equal ability of each technique to detect the changes of surface potential. The data imply no electrostatically detectable rearrangement of the interface in these instances. The discrepancy between the methods may occur at high ionic strength (Fig. 1) due to the inequality of the shear plane to the physical boundary. This deviation of the ζ-potential from the boundary potential allowed for independent verification of the shear plane distance (parameter δ), which is commonly used for quantitative analysis of electrophoretic data obtained in phospholipid liposomes (Eisenberg et al., 1979; McLaughlin, 1989).

The electrostatic effects were treated in the framework of the GCS model, with the assumptions of 1:1 binding stoichiometry and competition between the cations. All data were fit satisfactorily with the same set of principle parameters of the model, which includes binding constants for all cations and the surface density of binding sites. (The parameters K and S are not completely independent in the fitting procedure [see Fig. 1, *curves 2–4*]. Indeed, at low occupancies, the surface charge density, σ, in Eq. A7 is proportional to the product $K \times S$. The problem of adequate fitting of data for monovalent cations is discussed in Ermakov (1990). For calculations, we choose $S = 0.2$ C/m^2, which corresponds to the maximal stoichiometry of binding, one ion per one lipid [McLaughlin et al., 1981; Westman et al., 1984]). Our data do not pose any reason to suspect that we deal with gadolinium complexes of variable valence or that the affinity of binding sites changes with their density or occupancy. We have explained quantitatively the high slope of ϕ_s isotherms observed in the micromolar range of concentrations as the effect of bulk depletion of the cations possessing exceptionally high-affinity to the negatively charged surface of PS. A similar effect of depletion was mentioned for electrokinetic measurements of PS liposomes in the presence of La^{3+} (Bentz et al., 1988). The quantitative description of depletion required only one adjustable parameter c_{lip}, which was not essential for the evaluation of the magnitude of dipole effects.

It is commonly accepted that, due to the intrinsic dipole potential, the core of phospholipid membranes is 200–300 mV more positive relative to the boundary layer of electrolyte (Andersen et al., 1976; Flewelling and Hubbell, 1986; Tocanne and Teissie, 1990). We could not find any reference in the literature on the magnitude of the dipole potential for membranes made specifically of PS. Our data indicate that Gd^{3+} bound to PS may either decrease or increase the intrinsic dipole potential. We consistently see a decrease of the dipole potential either at low PS content in the membrane-forming mixture, at low pH (Figs. 5 and 6), or at low occupancy of binding sites (Figs. 6 and 7). At high PS content and high occupancies by the ion, we observe an appreciable increase of the intrinsic ϕ_d in the presence of Be^{+2} (+30 mV), and a very strong positive dipole effect of Gd^{+3} (+140 mV), indicative of restructuring of the surface. The strong dipole effect clearly correlates with the increase in membrane tension (Fig. 8) and transversal rigidity, suggesting the change in lipid packing confirmed in monolayer experiments (Yu. A. Ermakov, V. L. Shapovalov, and S. Sukharev, in preparation). Evidently, the altered bilayer structure may change other properties, such as viscosity and diffusion coefficients for lipids and other substances inside the membrane, which argues against the use of lipophilic ions for dipole potential measurements in these instances. Rigidification of the bilayer may lead to significant errors in ϕ_d estimation.

Our observations of negative dipole effects are consistent with the potency of many cations to dehydrate the membrane surface. Water molecules oriented by the phosphate and carbonyl groups of phospholipids augment the outwardly directed dipole contribution of carbonyls (Gawrisch et al., 1992). A removal of water, therefore, is predicted to diminish the intrinsic dipole potential. For instance, Li^+ causes substantial dehydration of phosphate and carbonyl groups of PS headgroups, which, in pure synthetic lipids, is typically associated with isothermal liquid–gel phase transitions (Hauser, 1991). Peculiarly, Mg^{2+} and Ca^{2+}, which also increase the melting temperature, cause less dehydration, reducing the amount of water near the phosphate groups of PS only (Hubner et al., 1994). Our measurements on bovine PS showed no dipole effect of Mg^{2+}, in contrast to the high-affinity cations of Be^{2+} and Gd^{3+}. Previously, using the same approach, we found that, during the phase transition in DPPC membranes in the presence of Be^{2+}, $\Delta\phi_b$ and $\Delta\phi_s$ have opposite signs, indicating the decrease of the intrinsic dipole potential consistent with the predicted effect of dehydration. Noticeable isotope effects on the ζ-potentials and phase transition temperature shifts induced by Be^{2+} observed on DPPC liposomes in D_2O support the same conclusion (Ermakov et al., 1994).

The difference in the behavior of PS and PC in the presence of ions can be accounted for by the chemistry of their headgroups. The dipole potential at the surface of PC membrane is attributed to the presence of two carbonyl groups, the P^-–N^+ phosphocholine group and oriented water typically hydrating the *sn*-2 carbonyl and the phosphate group (Gawrisch et al., 1992). In PS, there is additional an negatively charged carboxyl group with its own dipole moment. We demonstrated the critical role of the ionized form of PS in the generation of the positive dipole effect, pointing to the primary role of these carboxyls. However, at the present stage, we cannot conclude whether the dipole moments of carboxyls only, or of other groups as well, contribute to the gross dipole potential changes resulted from the high-affinity ion adsorption. The high-magnitude positive dipole effect appears to result from concerted interactions of more than one adjacent PS headgroup. The onset of the effect occurs at Gd^{3+} concentration near the zero charge point, i.e., when three PS headgroups coordinate one Gd^{3+} ion.

Pettersheim and Sun (1989) have shown that lanthanide ions are coordinated within a layer of PS molecules by both phosphates and carboxyls. This makes possible a cross-linking of the PS sheet, because one lanthanide ion may coordinate three PS molecules, whereas each PS may potentially interact with two different ions. The authors observed a stronger conformational effect in the inner, more compressed leaflet of liposomes and proposed that the lanthanide-induced "conformational change is not a direct consequence of forming the cation–PS complex, but appears to be a more delocalized effect of the cation headgroup pack-

ing, i.e., electrostatic repulsion of the serine ammonium group." We infer that this delocalized effect may be due to a strong condensation of the lipid layer, a decrease of the area per headgroup and a resulting electrostatic or steric conflict between the headgroups, which forces the conformation to change. Importantly, in our experiments, the subsequent dipole rearrangement, not the binding parameters for Gd^{3+}, critically depends on the density of ionized PS groups. Consistent with the inference that the dipole effect is a result of lipid condensation, a compression of dimirystoyil PS monolayers to ~30 mN/m (with no Gd^{3+} in the subphase) is found to increase the dipole potential an additional 100 mV, comparable to the dipole effect of Gd^{3+} (Yu. A. Ermakov, V. L. Shapovalov, and S. Sukharev, in preparation). The observed electrostatic effects do not provide information on the exact conformation assumed by the PS headgroup in the presence of Gd^{3+}, but the sign and magnitude of the total dipole potential change (+170 mV, accounting for −30 mV due to dehydration) suggest that positively charged amino groups move to a certain depth toward the membrane interior, and stay behind the layer of phosphates, possibly forming hydrogen bonds with dehydrated carbonyls. The negatively charged carboxyls in this conformation are likely to remain on the periphery.

The observed interaction of Be^{2+} ($K = 10^3\ M^{-1}$) and Gd^{3+} ($K = 5 \cdot 10^4\ M^{-1}$) with PS correlates with the broad spectrum of membranotropic effects of these ions in model systems, and in vivo. Be^{2+} is the smallest of all divalent ions with the charge density ($z/r = 5.66$) similar to that of some trivalents. It induces membrane rigidification and phase separation with a potency comparable to that of Al^{3+}, Ga^{3+}, In^{3+}, and Sc^{3+} (Verstraeten et al., 1997). Long known for its high toxicity, the inhaled beryllium (or BeO) dust causes immune-mediated lesions in lungs (chronic beryllium disease), associated with lymphocyte infiltration and aggregation of macrophages (Finch et al., 1998). It has also been established recently that macrophages specifically recognize PS in the outer leaflet of the cells undergoing apoptosis, and the lipid in these cases is the signal that triggers phagocytosis (Fadok et al., 1998, 2000). It seems logical to propose that Be^{2+} somehow promotes the accumulation of PS on the outer surface of a normal epithelium, which is then attacked by phahgocytes. The questions of whether the putative redistribution of PS takes place in the presence of Be^{2+} and whether it is mediated by physical lipid clusterization by the ion, by promoting nonspecific flip-flop, activation of scramblase, or by blockage of specific aminophospholipid translocase (Bratton et al., 1997), are pertinent in this context.

Gd^{3+}, a "small" lanthanide, actively displaces Ca^{2+} from the surface of neutral PC membranes and causes fatty acid chain ordering and phase separation (Li et al., 1994). Its effects range from inhibition of gravitropism in plant roots (Millet and Pickard, 1988), blockage of various mechanogated channels (Yang and Sachs, 1989; Hamill and McBride, 1996; Oliet and Bourque, 1996), to inhibition of hemagglutinin-mediated cell fusion (L. Chernomordik, personal communication) and lipid clusterization and pore formation in erythrocytes (Cheng et al., 1999).

This work and the preceding studies (Bentz et al., 1988) show that PS polar moeities may act as ubiquitous nonspecific receptors for lanthanide ions in native membranes. The lipid ordering, rigidification, and phase separation induced by the ions may directly effect membrane-embedded proteins. The increase of membrane tension and decrease of transversal compliance reported here suggest that the change of mechanical properties of the bilayer does take place in the presence of Gd^{3+}. Mechanosensitive channels are the most likely proteins that are sensitive to such perturbations. In the event of phase separation, mechanosensitive channels embedded in "frozen" lipid domains may be mechanically isolated from the tension-transducing fluid part of the membrane and, thus, may turn insensitive to stretch. Under normal conditions, when such channels are activated by tension, their proteins expand in the plane of the membrane (Sukharev et al., 1999). The condensation of surrounding lipids in the presence of Gd^{3+} may exert positive pressure on the proteins, which would oppose the conformational transition favored by tension. Another attractive hypothesis is that Gd^{3+}-induced lipid condensation may change the pressure profile across the lipid bilayer (Cantor, 1999), thus biasing the conformation of the transmembrane domains in certain proteins toward the closed state. The questions on the magnitude of pressure that can be generated by ion binding, the conformation of polar headgroups, the state of hydrocarbon chains under such conditions, and the effects on lipid-embedded proteins outline the scope of problems for future research.

APPENDIX

Surface potential: quantitative analysis of electrokinetic data and ionic equilibria

The measured electrophoretic mobility of liposomes μ is related to viscosity, η, and dielectric properties of the medium by the Smoluchowsky equation,

$$\mu = \frac{\zeta \varepsilon \varepsilon_0}{\eta}. \tag{A1}$$

The ζ-potential refers to the shear plane, the distance to which from the charged surface, δ, is generally unknown. For phospholipid liposomes, the best correspondence between the theory and experimental observations was achieved with $\delta = 0.2$ nm (McLaughlin, 1989). The data of Fig. 1 and their analysis provide independent support to this estimate. The potential at the surface $\phi(0) = \phi_s$ can be determined from the ζ-potential. When $\zeta <$ 25 mV and the ionic strength is low (<10 mM), the difference between ζ-potential and ϕ_s is negligibly small (1–2 mV). In all other cases, correction is required (McLaughlin, 1989). In the framework of the Gouy–Chapman model for symmetrical electrolytes, the distribution of electric potential in the diffuse part of the double layer satisfies the equation

(Hunter, 1981),

$$\tanh\left(\frac{ez\phi(x)}{4kT}\right) = \exp(-\kappa x)\tanh\left(\frac{ez\phi(0)}{4kT}\right), \qquad \text{(A2)}$$

where $\kappa = \sqrt{2e^2c/\varepsilon\varepsilon_0 kT}$ is inverse Debye length. However, when the electrolyte contains ions of different valence, Eq. A2 is used only as an approximation. In these instances, the valence z is substituted with the valence of a dominant counterion, and the concentration c is replaced with the ionic strength, $I = 0.5\ \Sigma_1\, c_{1,\mathrm{bulk}} z_1^2$. Previously, we have shown that the error between such approximation and the exact numerical solution of the Poisson–Boltzmann equation for $\delta = 0.2$ nm does not exceed 10 mV in a wide range of ion concentrations (Ermakov et al., 1992).

In a symmetrical binary electrolyte, the surface charge density can be calculated from the surface potential, $\phi(0)$, using the conventional Gouy–Chapman equation,

$$\sigma = \sqrt{8kT\varepsilon\varepsilon_0 c_{\mathrm{bulk}}}\,\sinh\left(\frac{ez\phi(0)}{2kT}\right). \qquad \text{(A3)}$$

For more complex electrolytes, the relationship between the surface charge and potential is given by the formula introduced by Grahame (1947),

$$\sigma^2 = 2kT\varepsilon\varepsilon_0 \sum_i c_{i,\mathrm{bulk}}\left[\exp\left(-\frac{ez_i\phi(0)}{kT}\right) - 1\right]. \qquad \text{(A4)}$$

Both Eqs. A3 and A4 account for the effect of surface charge screening and connect the surface potential with the ionic composition of electrolyte, assuming that the concentration of ions by the surface, c_i, is related to the bulk concentration with the Boltzmann relationship,

$$c_1(x) = c_{i,\mathrm{bulk}}\exp(-ez_i\phi(x)/kT), \qquad \text{(A5)}$$

where $c_{i,\ \mathrm{bulk}}$ is the bulk concentration of ions, z_I is the valence, and $\phi(x)$ is the potential at the distance χ from the surface, e is the electron charge. The surface charge is determined by the adsorbed ions, so, the Gouy–Chapmen–Stern model is combined with the Langmuir isotherm. Taking into consideration the competitive binding of two types of cations to negative singly charged binding sites, the total surface charge density can be expressed as

$$\frac{\sigma}{S} = \frac{(z_2 - 1)K_2c_2}{1 + K_1c_1 + K_2c_2} - \frac{1}{1 + K_1c_1 + K_2c_2}. \qquad \text{(A6)}$$

The equation presents the normalized surface charge density as a sum of two terms: the first is proportional to the occupancy of binding sites by cations (Θ), whereas the second is proportional to the density of unoccupied negative binding sites. It includes concentrations of monovalent (c_1) and multivalent (c_2) cations near the surface and their binding constants, K_1 and K_2, respectively (McLaughlin et al., 1981).

If the binding sites are initially uncharged (as on a neutral PC membrane), the contribution of monovalent cations in most cases is negligibly small and the isotherm includes only the binding of multivalent cations of valence z_2 (McLaughlin et al., 1978),

$$\frac{\sigma}{S} = \frac{z_2K_2c_2(0)}{1 + K_2c_2(0)}. \qquad \text{(A7)}$$

Here and below, we assume the 1:1 binding stoichiometry of one cation per one lipid headgroup. The maximal density of binding sites, S, in Eqs. A6 and A7 is expressed in units of charge density. We use $S = 0.2$ C/m^2 corresponding to the area of approximately 0.6 nm^2 per lipid molecule.

The use of the above equations is straightforward when the bulk concentrations of ions are well defined in the experiment. However, if the volume of the experimental chamber is small while the charged surface is large, c_{bulk} may significantly deviate from the total amount of introduced ions relative to the chamber volume, c_{tot}. The effect of bulk depletion in these instances should be accounted with the mass balance condition,

$$c_{\mathrm{tot}} = c_{\mathrm{bulk}} + c_{\mathrm{dif}} + c_{\mathrm{ads}}, \qquad \text{(A8)}$$

where c_{dif} and c_{ads} are the amounts of ions in the diffuse double layer and ions bound to the surface, respectively, each divided by the total volume of the chamber, V (Ermakov et al., 1997). The surface excess of ions in the diffuse double layer near the charged surface of total area A can be defined as

$$\frac{c_{\mathrm{dif}}}{c_{\mathrm{bulk}}} = \Omega\,\frac{A}{V}. \qquad \text{(A9)}$$

Here, Ω is the excess of ions in the double layer per unit area. It can be found using the Boltzmann relationship (Eq. A5) and the profile of electric potential along the x axis normal to the surface (Eq. A2):

$$\Omega = \int\left(\frac{c(x)}{c_{\mathrm{bulk}}} - 1\right)\mathrm{d}x. \qquad \text{(A10)}$$

On assumption that the total lipid concentration in the chamber, c_{lip}, and every molecule contributes to the surface and is accessible for ions, the A/V ratio in Eq. A9 can be calculated as $N_A \cdot A_{\mathrm{lip}} \cdot C_{\mathrm{lip}} \cdot 1000 = 6.4 \cdot 10^8\ c_{\mathrm{lip}}$ (M^{-1}). In a typical liposome suspension used in electrophoretic experiments, c_{lip} was approximately 1 mM.

The work was supported by INTAS (#96-1310), the Russian Foundation for Basic Research (#00-04-48920) to Y.A.E., and in part by the National Aeronautics and Space Administration (NAG2-1352) to S.S.

REFERENCES

Alvarez, O., and R. Latorre. 1978. Voltage-dependent capacitance in lipid bilayers made from monolayers. *Biophys. J.* 21:1–17.

Andersen, O. S., A. Finkelstein, I. Katz, and A. Cass. 1976. Effect of phloretin on the permeability of thin lipid membranes. *J. Gen. Physiol.* 67:749–771.

Babakov, A. V., L. N. Ermishkin, and E. A. Liberman. 1966. Influence of electric field on the capacity of phospholipid membranes. *Nature.* 210: 953–955.

Bentz, J., D. Alford, J. Cohen, and N. Duzgunes. 1988. La^{3+}-induced fusion of phosphatidylserine liposomes. Close approach, intermembrane intermediates, and the electrostatic surface potential. *Biophys. J.* 53: 593–607.

Boggs, J. M. 1987. Lipid intermolecular hydrogen bonding: influence on structural organization and membrane function. *Biochim. Biophys. Acta.* 906:353–404.

Bratton, D. L., V. A. Fadok, D. A. Richter, J. M. Kailey, L. A. Guthrie, and P. M. Henson. 1997. Appearance of phosphatidylserine on apoptotic cells requires calcium- mediated nonspecific flip-flop and is enhanced by loss of the aminophospholipid translocase. *J. Biol. Chem.* 272: 26159–26165.

Cantor, R. S. 1999. Solute modulation of conformational equilibria in intrinsic membrane proteins: apparent "cooperativity" without binding. *Biophys. J.* 77:2643–2647.

Carius, W. 1977. Studies of nonlinear electrical effects of model membranes. *Biophys. Struct. Mech.* 3:327–328.

Cheng, Y., M. Liu, R. Li, C. Wang, C. Bai, and K. Wang. 1999. Gadolinium induces domain and pore formation of human erythrocyte membrane: an atomic force microscopic study. *Biochim. Biophys. Acta.* 1421:249–260.

Cherny, V. V., V. S. Sokolov, and I. G. Abidor. 1980. Determination of surface charge of bilayer lipid membranes. *Bioelectrochem. Bioenerg.* 7:413–420.

Eisenberg, M., T. Gresalfi, T. Riccio, and S. McLaughlin. 1979. Adsorption of monovalent cations to bilayer membranes containing negative phospholipids. *Biochemistry.* 18:5213–5223.

Ermakov, Yu. A. 1990. The determination of binding site density and association constants for monovalent cation adsorption onto liposomes made from mixtures of zwitterionic and charged lipids. *Biochim. Biophys. Acta.* 1023:91–97.

Ermakov, Yu. A., A. Z. Averbakh, and S. I. Sukharev. 1997. Lipid and cell membranes in the presence of gadolinium and other ions with high affinity to lipids. 1. Dipole and diffuse components of the boundary potential. *Membr. Cell Biol.* 11:539–554.

Ermakov, Yu. A., V. V. Cherny, and V. S. Sokolov. 1992. Adsorption of beryllium on neutral and charged lipid membranes. *Biol. Membrany.* 6:254–272 (English translation).

Ermakov, Yu. A., V. V. Cherny, V. S. Sokolov, and S. A. Tatulian. 1983. Boundary potentials in lipid membranes in the presence of 1-anilino-8-naphthalenesulfonate ions. *Biofizika.* 28:1074–1078.

Ermakov, Yu. A., S. S. Makhmudova, E. V. Shevchenko, and V. I. Lobyshev. 1994. Effect of beryllium on the electrostatic and thermodynamic properties of dipalmitoyllecithin membranes. *Biol. Membrany*. 7:199–212 (English translation).

Fadok, V. A., D. L. Bratton, S. C. Frasch, M. L. Warner, and P. M. Henson. 1998. The role of phosphatidylserine in recognition of apoptotic cells by phagocytes. *Cell Death. Differ.* 5:551–562.

Fadok, V. A., A. de Cathelinau, D. L. Daleke, P. M. Henson, and D. L. Bratton. 2000. Loss of phospholipid assymmetry and surface exposure of phosphatidylserine is required for phagocytosis of apoptotic cells by macrophages and fibroblasts. *J. Biol. Chem.* In press.

Finch, G. L., K. J. Nikula, and M. D. Hoover. 1998. Dose-response relationships between inhaled beryllium metal and lung toxicity in C3H mice. *Toxicol. Sci.* 42:36–48.

Flewelling, R. F., and W. L. Hubbell. 1986. The membrane dipole potential in a total membrane potential model. Applications to hydrophobic ion interactions with membranes. *Biophys. J.* 49:541–552.

Gawrisch, K., D. Ruston, J. Zimmerberg, A. Parsegian, R. P. Rand, and N. Fuller. 1992. Membrane dipole potentials, hydration forces, and the ordering of water at membrane surfaces. *Biophys. J.* 61:1213–1223.

Graham, I., J. Gagne, and J. R. Silvius. 1985. Kinetics and thermodynamics of calcium-induced lateral phase separations in phosphatidic acid containing bilayers. *Biochemistry.* 24:7123–7131.

Grahame, D. C. 1947. The electrical double layer and the theory of electrocapillarity. *Chem. Rev.* 41:441–501.

Hamill, O. P., and D. W. McBride, Jr. 1996. The pharmacology of mechanogated membrane ion channels. *Pharmacol. Rev.* 48:231–252.

Hammoudah, M. M., S. Nir, T. Isac, R. Kornhouser, T. P. Stewart, S. W. Hui, and W. L. C. Vaz. 1979. Intreraction of La^{3+} with phosphatidylserine vesicles: binding, phase transition, leakage and fusion. *Biochim. Biophys. Acta.* 558:338–343.

Hauser, H. 1991. Effect of inorganic cations on phase transitions. *Chem. Phys. Lipids* 57:309–325.

Hianik, T., and V. I. Passechnik. 1995. Bilayer Lipid Membranes: Structure and Mechanical Properties. Kluwer Academic Publishers, Ister Science, Bratislava, Slovakia.

Hubner, W., H. H. Mantsch, F. Paltauf, and H. Hauser. 1994. Conformation of phosphatidylserine in bilayers as studied by Fourier transform infrared spectroscopy. *Biochemistry.* 33:320–326.

Hunter, R. J. 1981. Zeta Potential in Colloid Science. Principles and Applications. Ottewill, R. H. and Rowell, R. L., editors. Colloid Science. Academic Press, London.

Leikin, S. L. 1985. Thermal fluctuations and capacity of bilayer lipid membranes in the electric field. *Biol. Membrany.* 2:82–831 (English translation).

Li, X., Y. Zhang, J. Ni, J. Chen, and F. Hwang. 1994. Effect of lanthanide ions on the phase behaviour of dipalmitoylphosphatidylcholine multilamellar liposomes. *J. Inorg. Biochem.* 53:139–149.

McLaughlin, A., C. Grathwohl, and S. G. A. McLaughlin. 1978. The adsorption of divalent cations to phosphatidylcholine bilayer membranes. *Biochim. Biophys. Acta.* 513:338–357.

McLaughlin, S. 1989. The electrostatic properties of membranes. *Annu. Rev. Biophys. Biophys. Chem.* 18:113–136.

McLaughlin, S., N. Mulrine, T. Gresalfi, G. Vaio, and A. McLaughlin. 1981. Adsorption of divalent cations to bilayer membranes containing phosphatidylserine. *J. Gen. Physiol.* 77:445–473.

Millet, B., and B. G. Pickard. 1988. Gadolinium ion is the inhibitor suitable for testing the putative role of stretch-activated ion channel in geotropism and thigmotropism. *Biophys. J.* 53:155 (Abstract)

Oliet, S. H. R., and C. W. Bourque. 1996. Gadolinium uncouples mechanical detection and osmoreceptor potential in supraoptic neurons. *Neuron.* 16:175–181.

Passechnik, V. I., and T. Gianik. 1978. Evaluation of the elasto-viscous properties of biological membranes from measurements on bilayers. *Biophysics.* 23:1020–1026.

Petersheim, M., and J. Sun. 1989. On the coordination of La^{3+} by phosphatidylserine. *Biophys. J.* 55:631–635.

Sawyer, R. T., V. A. Fadok, L. A. Kittle, L. A. Maier, and L. S. Newman. 2000. Beryllium-stimulated apoptosis in macrophage cell lines. *Toxicology.* 149:129–142.

Schoch, P., D. F. Sargent, and R. Schwyzer. 1979. Capacitance and conductance as tools for the measurement of asymmetric surface potentials and energy barriers of lipid bilayer membranes. *J. Membr. Biol.* 46:71–89.

Shimane, C., V. I. Passechnik, S. El-Karadagi, V. A. Tverdislov, N. S. Kovaleva, N. V. Petrova, I. G. Kharitonenkov, and O. V. Martzenyuk. 1984. Changes of electrical and viscousielastic properties of bilayer lipid membranes in their interaction with proteins and lipoproteins. *Biophysics.* 29:459–464.

Sokolov, V. S., and S. G. Kuzmin. 1980. Measurements of the difference in the surface potentials of bilayer membranes from the second harmonic of the capacitive current. *Biophysics* 25:174–177.

Sukharev, S. I., W. J. Sigurdson, C. Kung, and F. Sachs. 1999. Energetic and spatial parameters for gating of the bacterial large conductance mechanosensitive channel, MscL. *J. Gen. Physiol.* 113:525–540.

Tatulian, S. A. 1993. Ionization and ion binding. *In* Phospholipid Handbook. G. Cevc, editor. Marcel Dekker, New York. 511–553.

Tatulian, S. A. 1999. Surface electrostatics of biological membranes an ion binding. *In* Surface Chemistry and Electrochemistry of Membranes. T. S. Soersen, editor. Marcel Dekker, Inc., New York and Basel. 871–922.

Tocanne, J. F., and J. Teissie. 1990. Ionization of phospholipids and phospholipid supported interfacial lateral diffusion of protons in membrane model systems. *Biochim. Biophys. Acta.* 1031:111–142.

Uzgiris, E. E. 1978. Lazer Doppler methods in electrophoresis. *Progr. Surf. Sci.* 10:56–164.

Verstraeten, S. V., L. V. Nogueira, S. Schreier, and P. I. Oteiza. 1997. Effect of trivalent metal ions on phase separation and membrane lipid packing: role in lipid peroxidation. *Arch. Biochem. Biophys.* 338: 121–127.

Westman, J., L. E. G. Eriksson, and A. Ehrenberg. 1984. Interaction of the cationic form of amphiphilic drugs with phosphatidylcholine model membranes. Competition with lanthanide ions. *Biophys. Chem.* 19: 57–68.

Yang, X. C., and F. Sachs. 1989. Block of stretch-activated ion channels in *Xenopus* oocytes by gadolinium and calcium ions. *Science.* 243: 1068–1071.